論文 / 著書情報
Article / Book Information

Title	Transmission enhancement in rectangular-coordinate orthogonal multiplexing by excitation optimization of slot arrays for a given distance in the non-far region communication
Authors	Ryotaro Ohashi, Takashi Tomura, Jiro Hirokawa
Citation	IEICE TRANSACTIONS on Communications, vol. E103-B, no. 2, pp. 130-138
Pub. date	2020, 2
Copyright	Copyright (c) 2020 Institute of Electronics, Information and Communication Engineers.

IEICE TRANS. COMMUN., VOL.E103–B, NO.2 FEBRUARY 2020

PAPER

Transmission Enhancement in Rectangular-Coordinate Orthogonal Multiplexing by Excitation Optimization of Slot Arrays for a Given Distance in the Non-Far Region Communication

Ryotaro OHASHI[†a)], **Takashi TOMURA**[†], ***Members***, ***and*** **Jiro HIROKAWA**[†], ***Fellow***

SUMMARY This paper presents the excitation coefficient optimization of slot array antennas for increasing channel capacity in 2×2-mode two-dimensional ROM (rectangular coordinate orthogonal) transmission. Because the ROM transmission is for non-far region communication, the transmission between Tx (transmission) and Rx (reception) antennas increases when the antennas radiate beams inwardly. At first, we design the excitation coefficients of the slot arrays in order to enhance the transmission rate for a given transmission distance. Then, we fabricate monopulse corporate-feed waveguide slot array antennas that have the designed excitation amplitude and phase in the 60-GHz band for the 2×2-mode two-dimensional ROM transmission. The measured transmission between the fabricated Tx and Rx antennas increases at the given propagation distance and agrees with the simulation.

key words: *rectangular-coordinate orthogonal multiplexing, multiple-input multiple-output (MIMO), millimeter-wave antenna, munopulese circuit*

1. Introduction

The promising techniques for increase the transmission rate are moving to higher frequency bands and using multiplexing transmission. Various multiplexing techniques such as MIMO (multiple input multiple output) [1]–[5] and OAM (orbital angular momentum) [6]–[9] techniques using millimeter-waves are being widely researched. We are investigating the feasibility of ROM (rectangular-coordinate orthogonal multiplexing), a new multiplexing transmission antenna system for LOS (line of sight) short-range wireless communication in the millimeter wave band [10], [11]. ROM is a multiplexing technique that uses the orthogonality of the excitation polarities of the transmitting and the receiving antennas in rectangular-coordinate arrangement. It can be considered as equivalent to OAM transmission system using the orthogonality in the cylindrical-coordinate system in terms of space multiplexing. The OAM and the ROM transmissions are kinds of analog eigenmode transmission for short-range MIMO [12], [13]. Thanks to the introduction of symmetrical circuit components like magic-T's or E-plane T-junctions for the excitation polarities, the ROM transmission could communicate in a wider bandwidth than the OAM transmission with phase variation produced in the RF band that has typically a narrow bandwidth.

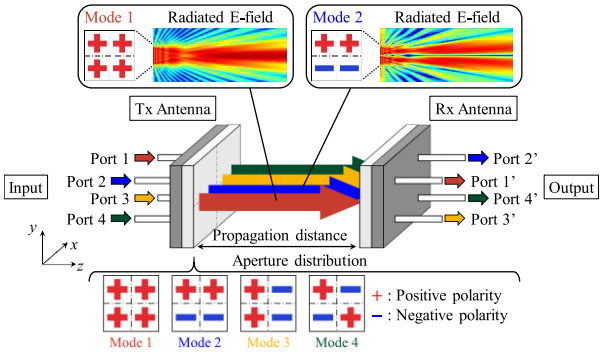

Fig. 1 2×2-mode ROM transmission antenna system.

Figure 1 shows the 2×2-mode two-dimensional ROM transmission antenna system [13]. The system uses two identical ROM antennas. The 2×2-mode multiplexing transmission is realized by exciting the antennas with combinations of positive and negative two-dimensional polarities as shown in Fig. 1. In order to receive these beams with the Rx (reception) antenna, the Tx (transmission) and Rx antennas are made to face each other in the non-far region.

In the ROM transmission antenna system, the transmission between the Tx and Rx antennas attenuates as the propagation distance increases due to the split beam divergence. The higher order mode with more polarity inversion, the larger the attenuation. This also occurs in OAM transmission system. In [11], the radiation field of the 2×2-mode ROM antenna and the transmission of the ROM transmission antenna system were measured using the fabricated antennas. The attenuation of the transmission by the radiation beam divergence in the higher order mode was observed experimentally. The problem is that transmission rate decreases as communication distance increases due to beam divergence and/or split in the ROM transmission antenna system, which is based on the orthogonality of the excitation over the antenna apertures in terms of polarity on as one of multiplexing transmission systems. In this work, we propose an excitation optimization to enhance the channel capacity at a given distance. This enables both larger capacity and longer communication distance simultaneously in the multiplexing transmission system.

To increase the transmission for a given distance, we propose a design of the excitation coefficients of the slot

Manuscript received February 26, 2019.
Manuscript revised June 3, 2019.
Manuscript publicized August 22, 2019.

[†]The authors are with the Department of Electrical and Electronic Engineering, Tokyo Institute of Technology, Tokyo, 152-8552 Japan.
a) E-mail: r.o_93_dia_jdg@icloud.com

DOI: 10.1587/transcom.2019EBP3051

array by using non-linear optimization in this paper. The increase of the transmission of each mode results in one way to enhance the channel capacity. The novelty of the work is the excitation optimization to enhance the channel capacity in the 2×2-mode ROM transmission antenna system for a given distance in the non-far region communication. A 16×16-element corporate-feed waveguide monopulse slot array antenna excited with the optimized excitation coefficients has been designed and fabricated for the ROM transmission antenna in the 60-GHz band. The effectiveness of the proposed excitation coefficient optimization has been demonstrated experimentally. Larger channel capacity than that by uniform excitation in the existing work has been achieved.

Another way to enhance the total capacity is to distribute properly a larger power for the mode with a larger transmission and to adopt higher-degree modulation scheme for the larger power. However, this paper is not discussed from this point of view to confirm the feasibility.

The paper is organized as follows. Section 2 analyzes the performance of the 2×2-mode ROM transmission antenna system. Section 3 optimizes the excitation coefficients of the array antenna to enhance the ROM transmission. Section 4 shows the ROM antenna architecture and the operation mechanism. Section 5 provides the experiment results of the fabricated ROM antenna that realized the optimized excitation coefficients and the ROM transmission antenna system. Finally, the effectiveness of the proposed design of the excitation coefficients is shown experimentally.

2. Multiplexing Transmission

2.1 Antenna System

An analysis model of the 2×2-mode ROM transmission antenna system assuming excitation distributions is shown in Fig. 2. The ROM antenna is a 16×16-element slot array antenna. The system is analyzed by replacing the array elements with infinitesimal small dipoles.

Figure 3 show four-mode excitation distributions excited with uniformly coefficients of the ROM antenna. The 16×16-element array is divided into four 8×8-element subarrays. Four orthogonal modes are formed by exciting each subarray with positive or negative polarities. In Fig. 3, the red parts show positive polarities and the blue parts show negative polarities. The four excitation distributions are orthogonal to each other.

2.2 Transfer Function of the System

The transfer function **H** of the 2×2-mode ROM transmission antenna system is given by Eq. (1).

$$\mathbf{H} = \begin{bmatrix} T_{11} & T_{12} & T_{13} & T_{14} \\ T_{21} & T_{22} & T_{23} & T_{24} \\ T_{31} & T_{32} & T_{33} & T_{34} \\ T_{41} & T_{42} & T_{43} & T_{44} \end{bmatrix} \tag{1}$$

The transfer function is composed of the transmission T_{rt}

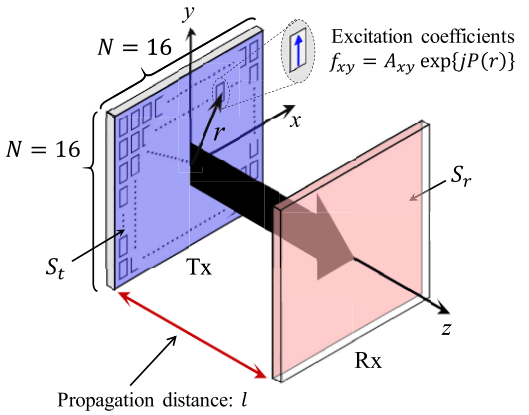

Fig. 2 Analysis model of transmission between two arrays.

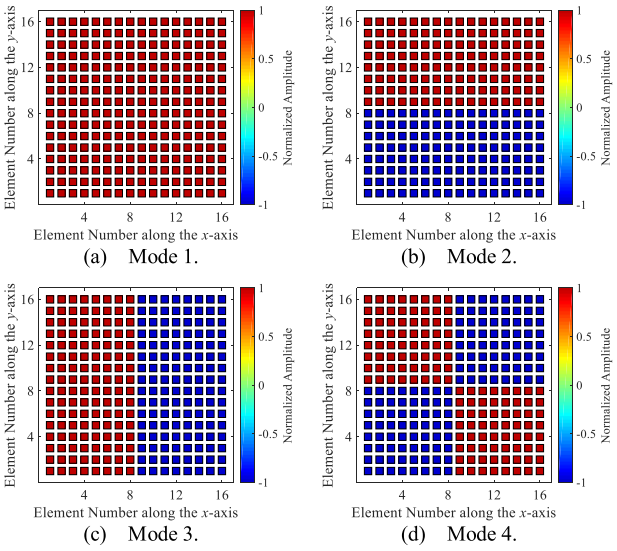

Fig. 3 Excitation distributions of four modes.

between the Tx and the Rx antennas like the S-matrix of the system. In the transmission T_{rt}, the subscripts t and r are the mode number of the Tx and Rx antennas, respectively. The same excitation coefficient distribution is used for the Tx and Rx antennas. When the values of r and t are different, the transmission is zero because of the orthogonal property among the modes in principle. **H** becomes a diagonal matrix. The transmission becomes larger as the radiating field on the reception plane by the Tx antenna gets close to the excitation distribution of the Rx antenna.

As the four modes are mutually orthogonal, the channel capacity of the system is the sum of channel capacities of individual four modes. The channel capacity of the system is given by Eq. (2).

$$\begin{aligned} C_{ROM} &= B \log_2 \left\{ \det \left(\mathbf{I} + \mathbf{H}^{\dagger} \frac{P_t}{N} \mathbf{H} \right) \right\} \\ &= \sum_{i=1}^{4} B \log_2 \left(1 + \frac{P_t}{N} |T_{ii}|^2 \right) \end{aligned} \tag{2}$$

where B is the bandwidth, P_t is the total transmission power, N is the received noise, and $\mathbf{A}^{\dagger}$ means the Hermitian conjugate of matrix $\mathbf{A}$.

3. Optimization of Excitation Coefficients

The excitation coefficients are designed to enlarge the transmission of the ROM transmission system. The excitation coefficients f_{xy} are expressed in amplitude A_{xy} and phase $P(r)$ $\left(r = \sqrt{x^2 + y^2}\right)$ as shown in Eq. (3).

$$f_{xy} = A_{xy} \exp\{jP(r)\} \tag{3}$$

Considering the symmetry of the structure, the design parameters are the amplitude and the phase of the 8×8-element subarray in one of the quadrants are designed. In view of the configuration of the antenna, the 2×2-element array is defined as the minimum radiation unit structure.

The normalized amplitude of each element is expressed by matrix $\mathbf{A}$ as Eq. (4). The diagonal elements are equalized $(A_{xy} = A_{yx})$.

$$\mathbf{A} = \begin{bmatrix} A_{11} & A_{12} & \cdots & A_{18} \\ A_{21} & A_{22} & \cdots & A_{28} \\ \vdots & \vdots & \ddots & \vdots \\ A_{81} & A_{82} & \cdots & A_{88} \end{bmatrix} \quad \left(0 \le A_{xy} \le 1\right) \tag{4}$$

The phase distribution is introduced a parabolic distribution from the center $(r = 0)$ to the edge $(r = R)$ of the aperture as given by Eq. (5). The parameter of the phase distribution is only ph.

$$P(r) = ph \times (r/R)^2 \quad (0 \le ph \le 2\pi) \quad \text{[rad.]} \tag{5}$$

The objective function to be maximized is determined that the product of the transmission of the four modes at a given propagation distance l_0 as follows:

$$f\left(f_{xy}, l_0\right) = \prod_{i=1}^{4} \left|T_{ii}\left(f_{xy}, l_0\right)\right| \tag{6}$$

Assuming the perfect orthogonal multiplexing transmission, the ROM transmission channel capacity is the sum of the four-mode capacities and is given by Eq. (7). In the non-far region, $\left(1 \ll P_t \left|T_{ii}\right|^2 / N\right)$ can be approximated. Since Eq. (7), maximizing the objective function Eq. (6) can be regarded as maximizing the ROM transmission channel capacity.

$$\begin{aligned} C_{ROM} &= \sum_{i=1}^{4} B \log_2 \left(1 + \frac{P_t}{N} \left|T_{ii}\right|^2\right) \\ &\cong \sum_{i=1}^{4} B \log_2 \left(\frac{P_t}{N} \left|T_{ii}\right|^2\right) \\ &\propto \log_2 \left(\prod_{i=1}^{4} \left|T_{ii}\right|\right) \end{aligned} \tag{7}$$

Table 1 Calculation and optimization conditions.

Frequency	61.5 GHz
Number of array elements	16×16 elements
Element spacing	0.83 wavelengths
Aperture size	64.8 mm × 64.8 mm
Propagation distances l_0	0.3 m, 0.4 m, 0.5 m

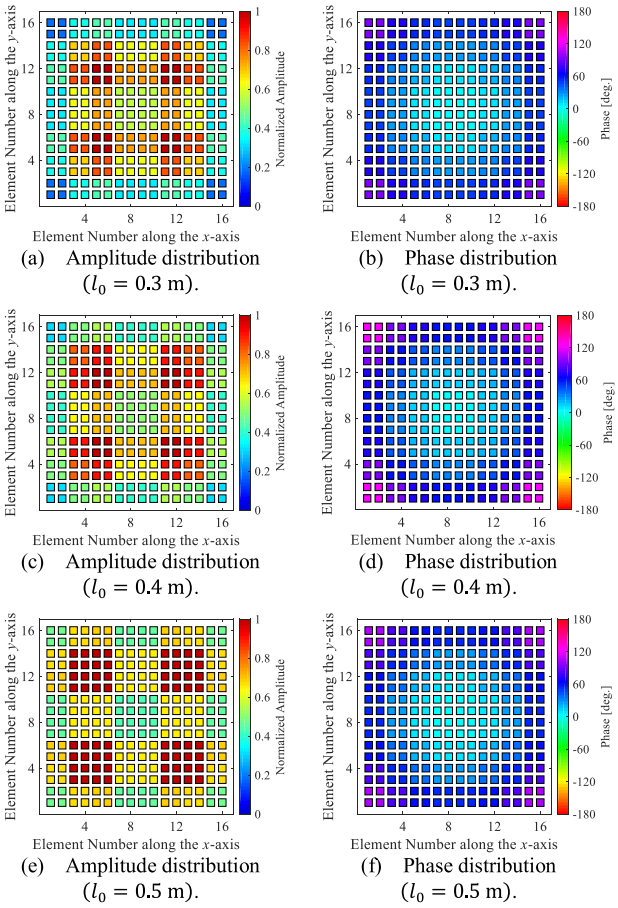

(a) Amplitude distribution ($l_0 = 0.3$ m).
(b) Phase distribution ($l_0 = 0.3$ m).
(c) Amplitude distribution ($l_0 = 0.4$ m).
(d) Phase distribution ($l_0 = 0.4$ m).
(e) Amplitude distribution ($l_0 = 0.5$ m).
(f) Phase distribution ($l_0 = 0.5$ m).

Fig. 4 Optimized excitation coefficients.

Results of the optimization design are provided. The conditions in the calculation and the optimization are shown in Table 1. The optimization is based on the interior-point method [14].

Figure 4 show the optimized excitation coefficient distribution with each value of l_0. The optimized amplitude distribution has four local maximum values in the aperture. When the given distance l_0 increases, the taper of the optimized amplitude distribution becomes gentler. The optimized phase distribution is progressing from the center to the edge of the aperture so that the beams are directed inward. The values of the optimized ph in Eq. (5) are 90 deg. for $l_0 = 0.3$ m, 120 deg. for $l_0 = 0.4$ m and 100 deg. for $l_0 = 0.5$ m. The optimized ph in Eq. (5) reaches its maximum value when $l_0 = 0.4$ m. The propagation distance that can be effectively used for each mode is limited by the

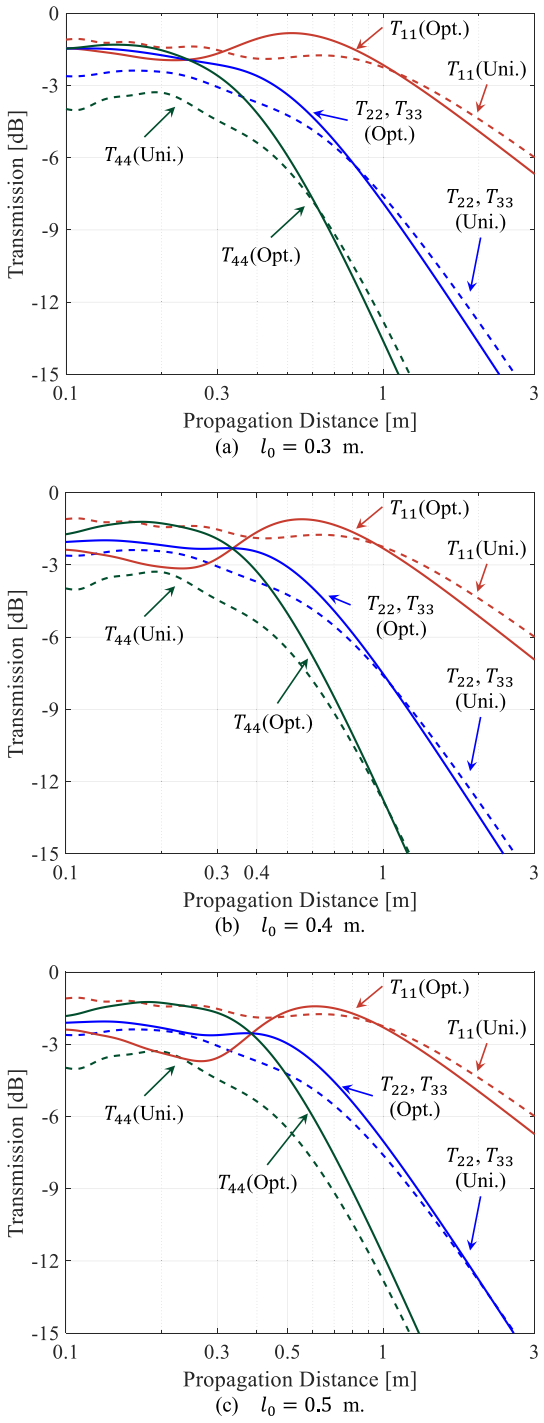

Fig. 5 Simulated propagation distance characteristics of transmission between same mode apertures.

aperture size of the antenna. Under the analysis condition, $l_0 = 0.4$ m is the maximum propagation distance that efficiently utilizes all four modes.

Figure 5 show the propagation distance characteristics of the transmissions for the optimized excitation coefficients given in Fig. 4. For comparison, those for the uniform amplitude excitation with the proper polarity are shown by the dashed lines.

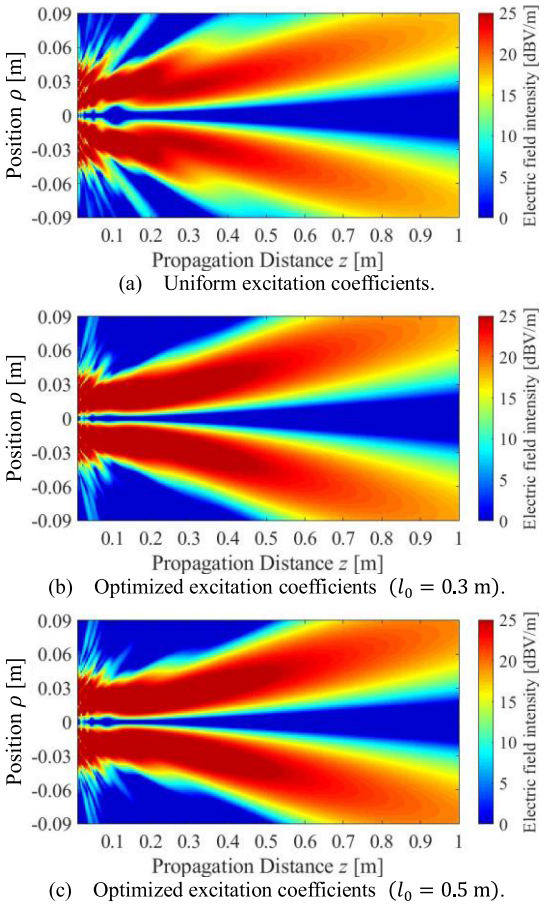

Fig. 6 Simulated near field distribution of mode 4 in the $\varphi = 45$ deg. plane.

The near-field distributions excited by mode 4 with uniform and optimized excitations in the $\varphi = 45$ deg. plane are shown in Fig. 6. ρ is the distance from z-axis in the $\varphi = 45$ deg. plane. The improvement of the transmission is realized by pointing radiated power inwardly and decreasing the leakage of the power. This is accomplished by controlling the amplitude and the phase in the excitations. As a result, the sidelobe decreases and beamwidth increases. The electrical field intensity by the optimized excitation is stronger than that by the uniform excitation in the range of $y = -0.32$ m–$+0.32$ m and $z = 0.3$ m or $z = 0.5$ m (the Rx antenna position). This means that radiated power is concentrated in the transmission axis in near-field.

The design objective is to maximize the product of the transmission coefficients in Eq. (7) and it is not to increase all the transmission coefficients by the optimized excitation. The improvement of each mode transmission is a trade-off with the same excitation amplitudes for all modes. Increasing the transmission of mode 4 is effective to maximize the objective function because mode 4 has smaller transmission than the other modes. The optimized excitation coefficients maximize the objective function by increasing the transmission of mode 4 and decreasing the transmission of mode 1 compared to the uniformly excitation.

The normalized channel capacity of the ROM trans-

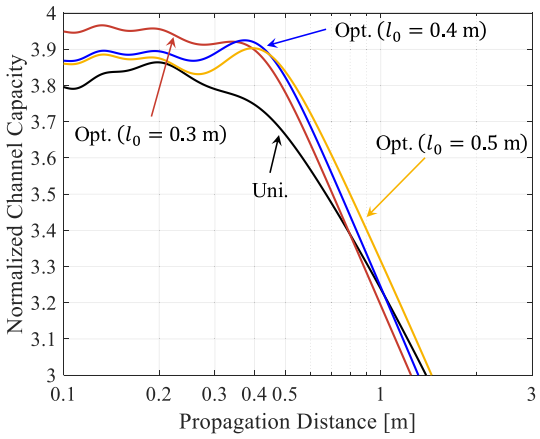

Fig. 7 Simulated propagation distance characteristics of normalized channel capacity.

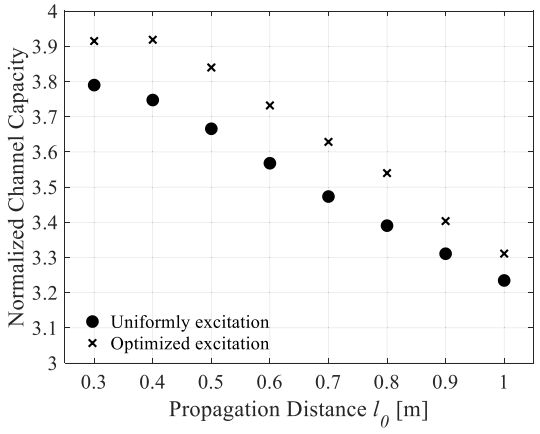

Fig. 8 Simulated propagation distance l_0 characteristics of normalized channel capacity.

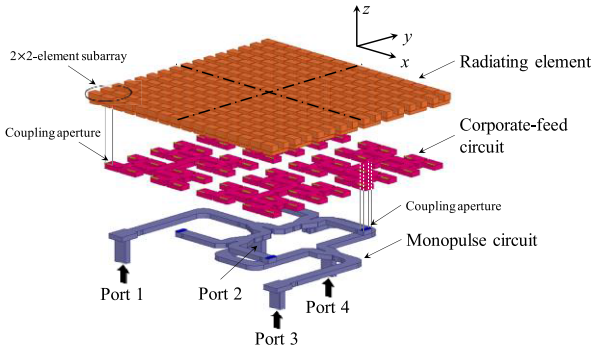

Fig. 9 ROM antenna configuration.

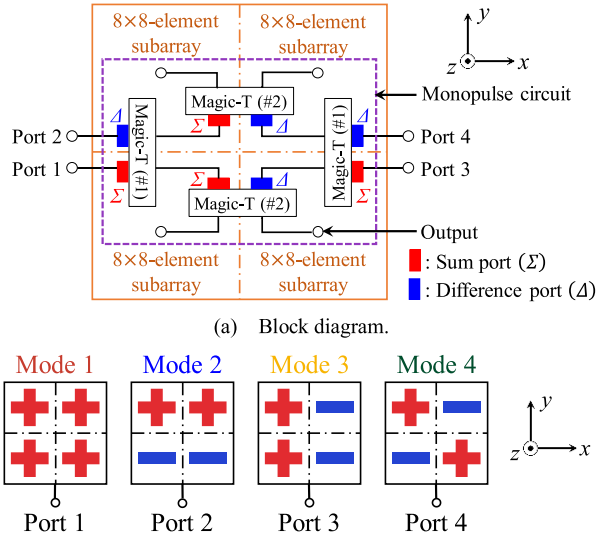

(a) Block diagram.

(b) Excitation polarities of the four subarrays.

Fig. 10 Operation mechanism of the ROM antenna.

mission system with respect to the channel capacity of SISO (single input single output) system is defined in this paper by Eq. (8).

$$\frac{C_{ROM}}{C_{SISO}} = \frac{\log_2\left\{\det\left(\mathbf{I}+\mathbf{H}^{\dagger}\frac{P_t}{N}\mathbf{H}\right)\right\}}{\log_2\left\{1+T_{11}(\text{Uni.})^{\dagger}\frac{P_t}{N}T_{11}(\text{Uni.})\right\}} \tag{8}$$

where $T_{11}(\text{Uni.})$ is the simulated transmission of mode 1 with uniformly excitation. Note that an equal power is assumed for all modes.

The propagation distance characteristics of the normalized channel capacity for an SNR equal to 30 dB is shown in Fig. 7. It can be confirmed that the normalized channel capacity is increased by designing the excitation coefficients for the propagation distance of l_0.

Figure 8 shows the normalized channel capacity at the propagation distance l_0 when the excitation coefficients are optimized at each of l_0. Figures 7 and 8 show that the normalized channel capacity with the uniformly excitation coefficients drops with increasing the propagation distance. This means that the ROM transmission system works efficiently in the non-far region of the antenna. In Fig. 8, the channel capacity of the 2×2-mode ROM transmission system with the optimized excitation coefficients is over 3.9 times larger than the channel capacity of the SISO system up to the propagation distance $l_0 = 0.4$ m. It is possible to reduce the leakage of the beam up to a certain distance by optimizing aperture distribution and confining the radiated power in transmission axis. However, it is not possible to reduce the leakage over this certain distance. The distance is determined by the antenna aperture size. In this paper, $l_0 = 0.4$ m is the most effective propagation distance for the given antenna size.

4. Multiplexing Transmission Antenna

We design a 2×2-mode ROM antenna excited with the optimized coefficients for the propagation distance $l_0 = 0.4$ m given in Figs. 4(c) and (d). The ROM antenna is composed of a corporate-feed waveguide slot array antenna and a monopulse circuit as shown in Fig. 9 [15]. The 16×16-element array is divided into four 8×8-element subarrays. Each of them is excited by a corporate-feed circuit. The optimized excitation coefficients are realized by the asym-

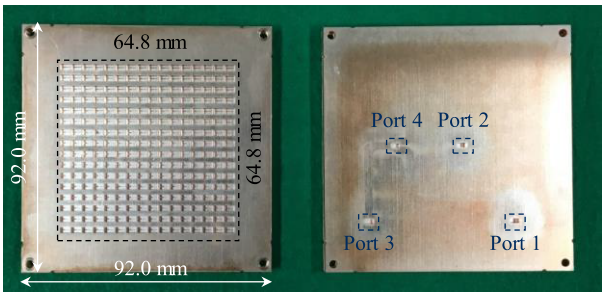

(a) Front side. (b) Back side.

Fig. 11 Fabricated antenna.

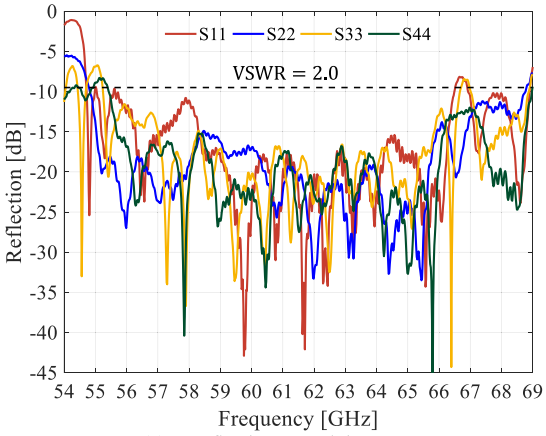

(a) Reflection at each input port.

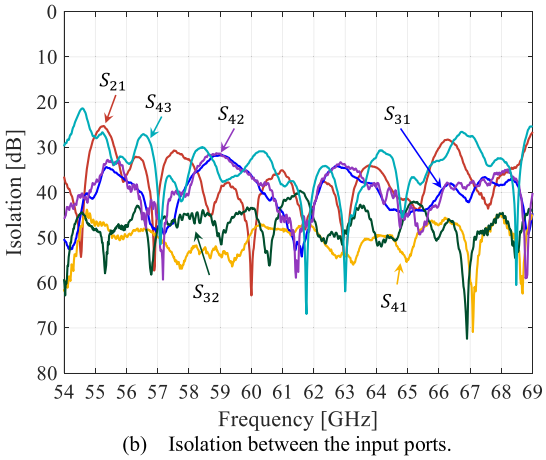

(b) Isolation between the input ports.

Fig. 12 Measured frequency characteristics.

metrical T-junctions in the corporate-feed circuit [16]. The four corporate-feed arrays are fed by the two-dimensional monopulse circuit composed of two-stage magic-T's.

Figure 10(a) shows a block diagram of the ROM antenna operation mechanism. The antenna has four input ports. Depending on the input ports, the excitation polarities of the four subarrays are controlled by the sum or the difference ports of the magic-T's as shown in Fig. 10(b).

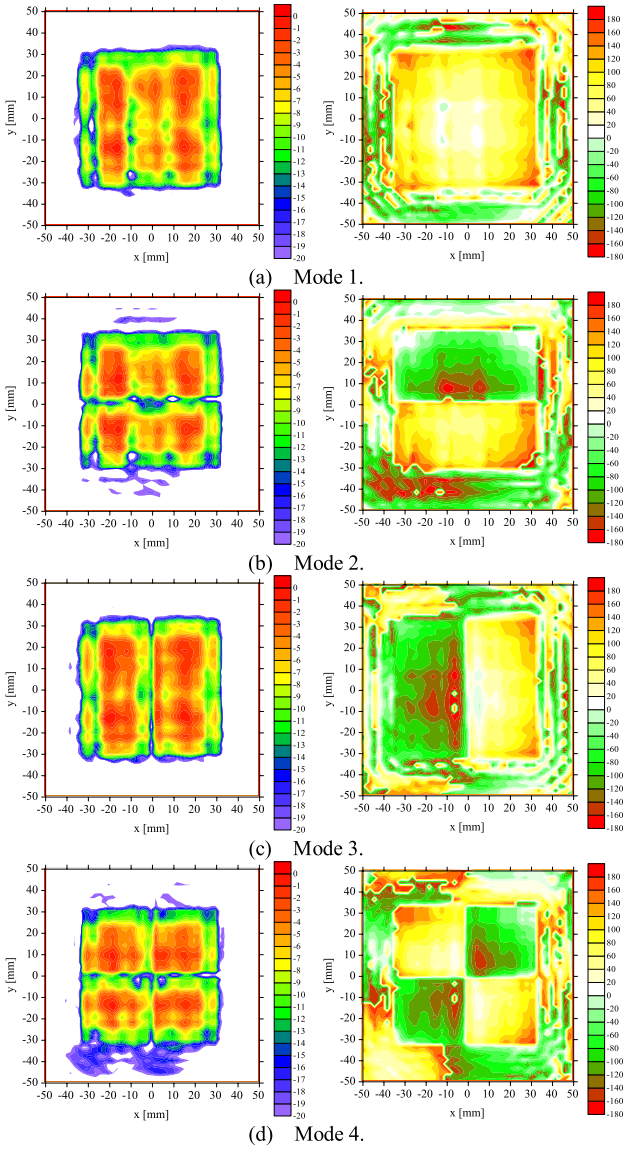

(a) Mode 1.
(b) Mode 2.
(c) Mode 3.
(d) Mode 4.

Fig. 13 Measured aperture field distributions at 61.5 GHz. Left: Normalized Amplitude distribution [dB]. Right: Phase distribution [deg.].

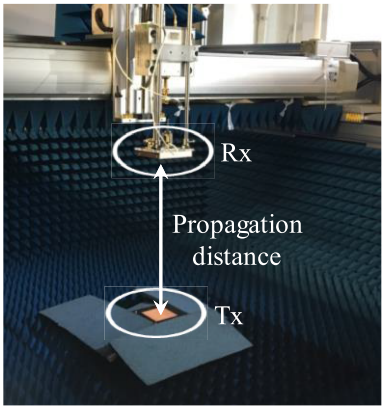

Fig. 14 Transmission measurement set-up.

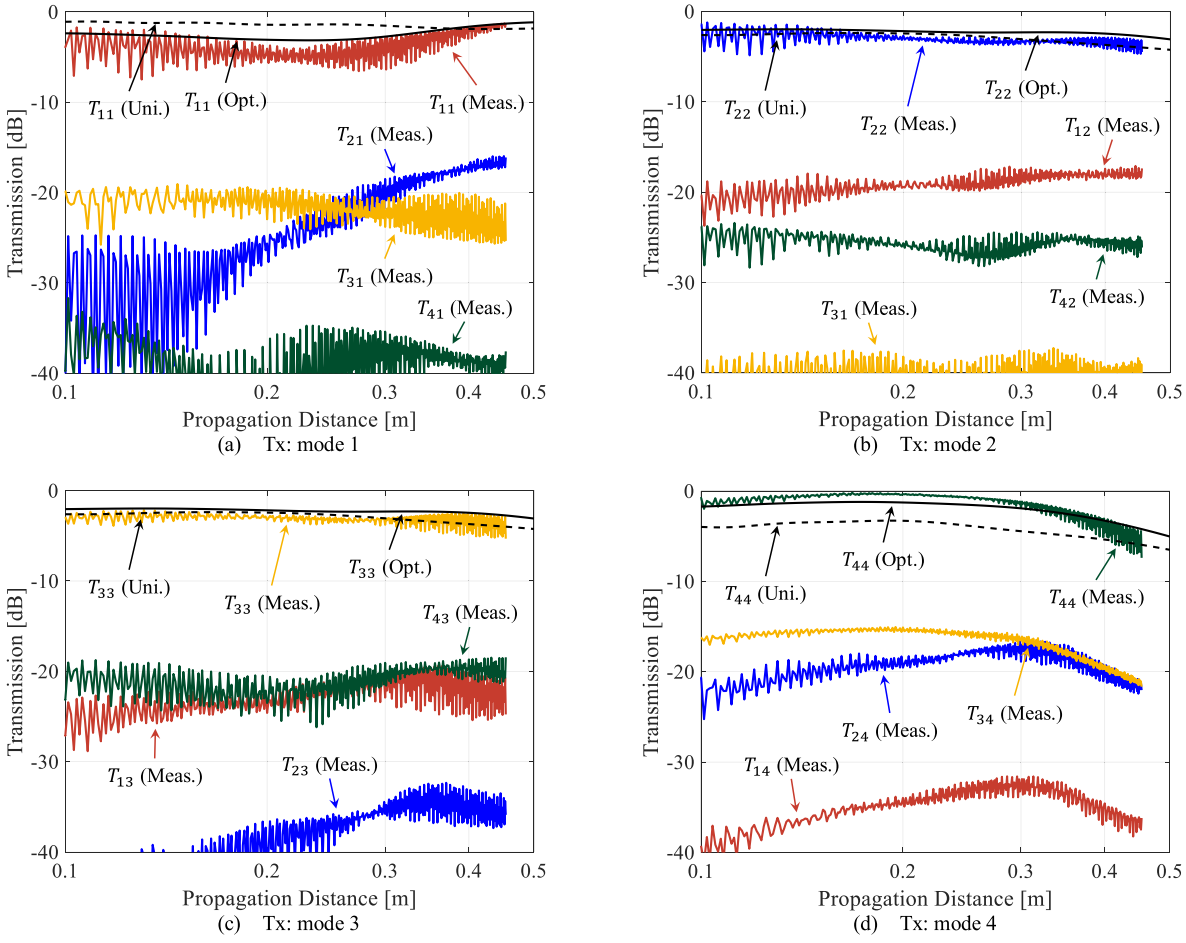

Fig. 15 Measured propagation distance characteristics of transmission between Tx and Rx antennas.

5. Experiment Results

A photo of the fabricated antenna is shown in Fig. 11. The dimensions of the antenna are 92.0 mm × 92.0 mm × 7.4 mm. The antenna is fabricated by the plate-laminated diffusion bonding technique [17], [18]. The antenna is fed by standard WR-15 waveguides (3.76 mm × 1.88 mm) from the back through the four input ports. The design frequency, the element spacing and the aperture size of the antenna are listed in Table 1.

5.1 Reflection and Isolation

Figure 12 show the measured frequency characteristics of the reflection and the isolation of the antenna. These results show a wide bandwidth and a high isolation in the 60-GHz band. The bandwidth of all the input ports for VSWR < 2.0 is 18.4% (55.3–66.5 GHz). In the design frequency, the isolation between two input ports are larger than 39.8 dB reflecting the structural symmetry of the magic-T.

5.2 Aperture Distribution

The measured aperture field distributions at the design frequency are shown in Fig. 13. The measured aperture field distributions of all the modes realize fairly the optimized excitation coefficient distributions given in Figs. 4(c) and (d). The measure amplitude distributions are slightly different among the modes because the mutual couplings among the elements could be changed by different mode excitation. The measured phase distributions are same polarity distributions as shown in Fig. 10(b).

5.3 Transmission between Tx and Rx Antennas

Figure 14 shows the transmission measurement set-up. Both the Tx and the Rx antennas are connected to a two-port vector network analyzer for the measurement of the S-matrix of the system. The measurement frequency is 61.5 GHz. The propagation distance between the Tx and the Rx antennas is changed from 0.10 m to 0.45 m.

Figure 15 show the measured propagation distance characteristics of the transmission between the Tx and the Rx antennas. In each of Fig. 15, the black dash line shows the

simulated transmission for uniform amplitude coefficients with proper polarity. The black solid line shows the simulated transmission with the optimized excitation coefficients. The color lines show the measured transmission between the Tx and the Rx antennas.

The measured transmissions between the desired modes $(T_{11}, T_{22}, T_{33}, T_{44})$ agree with the simulated ones. The measured isolation of transmissions between the desired mode and the different modes are larger than 14.7 dB at the propagation distance $l_0 = 0.4$ m. The ripple observed in the measured transmission is due to the multiple reflection between the antennas.

6. Conclusion

This study addressed excitation coefficient optimization to enhance the channel capacity of the 2×2-mode ROM transmission antenna system has been discussed. By designing the excitation amplitude and phase of the 16×16-element array antenna, the transmission rate between the two ROM antennas can be increased at any given propagation distance in the 60-GHz band.

We have designed and fabricated the monopulse corporate-feed waveguide slot array antennas excited with designed amplitude and phase as the 2×2-mode ROM transmission antennas. The bandwidth of all the input ports for measured VSWR < 2.0 is 18.4% (55.3–66.5 GHz) and the measured isolation between each input ports are larger than 39.8 dB in the design frequency.

The effectiveness of the proposed design method of excitation coefficients was demonstrated in experiments. The measured transmissions between the desired modes agree with the simulation. The measured isolation of transmissions between the desired mode and the different modes are larger than 14.7 dB at the propagation distance $l_0 = 0.4$ m.

References

[1] I.E. Telatar, "Capacity of multi-antenna Gaussian channels," Eur. Trans. Telecomm., vol.10, no.6, pp.585–595, Nov. 1999.
[2] T. Svantesson, "Correlation and channel capacity of MIMO systems employing multimode antennas," IEEE Trans. Veh. Technol., vol.51, no.6, pp.1304–1312, Nov. 2002.
[3] C. Waldschmidt and W. Wiesbeck, "Compact wide-band multimode antennas for MIMO and diversity," IEEE Trans. Antennas Propag., vol.52, no.8, pp.1963–1969, Nov. 2002.
[4] J. Sarrazin, Y. Mahé, S. Avrillon, and S. Toutain, "A new multimode antenna for MIMO systems using a mode frequency convergence concept," IEEE Trans. Antennas Propag., vol.59, no.12, pp.4481–4489, Dec. 2011.
[5] C.K.K. Jayasooriya, H.M. Kwon, S. Bae, and Y.-K. Hong, "Miniaturized multimode circular patch antennas for MIMO communications," Proc. IEEE Veh. Technol. Conf., Sept. 2009, DOI: 10.1109/VETECF.2009.5379071.
[6] G. Gibson, J. Courtial, and M.J. Padgett, "Free space information transfer using light beams carrying orbital angular momentum," Opt. Express, vol.12, no.22, pp.5448–5456, Nov. 2004.
[7] S.M. Mohammadi, L.K. S. Daldorff, J.E.S. Bergman, R.L. Karlsson, B.T.K. Forozesh, T.D. Carozzi, and B. Isham, "Orbital angular momentum in radio — A system study," IEEE Trans. Antennas Propag., vol.58, no.2, pp.565–572, Feb. 2010.
[8] O. Edfors and A.J. Hohansson, "Is orbital angular momentum (OAM) based radio communication an unexploited area?," IEEE Trans. Antennas Propag., vol.60, no.2, pp.1126–1131, Feb. 2012.
[9] A. Saitou, R. Ishikawa, and K. Honjo, "Four-value multiplexing orbital angular momentum communication scheme using loop antenna arrays," Asia Pacific Microw. Conf., Dec. 2016, DOI: 10.1109/APMC.2016.7931442.
[10] R. Ohashi, T. Tomura, and J. Hirokawa, "Feasibility on multiplexing antenna system based on rectangular-coordinate orthogonality by using two-dimensional 180-degree hybrid," Proc. Intl. Symp. Antennas Propag., Paper ID: 3E2-5, 2017.
[11] K. Tekkouk, J. Hirokawa, and M. Ando, "Multiplexing antenna system in the non-far region exploiting two-dimensional beam mode orthogonality in the rectangular coordinate system," IEEE Trans. Antennas Propag., vol.66, no.3, pp.1507–1515, March 2018.
[12] K. Murata, N. Honma, K. Nishimori, and H. Morishita, "Analog eigenmode transmission for short-range MIMO," IEEE Trans. Veh. Technol., vol.65, no.1, pp.100–109, Jan. 2016.
[13] K. Murata, N. Honma, K. Nishimori, N. Michishita, and H. Morishita, "Analog eigenmode transmission for short-range MIMO based on orbital angular momentum," IEEE Trans. Antennas Propag., vol.65, no.12, pp.6687–6702, Dec. 2017.
[14] R.H. Byrd, M.E. Hribar, and J. Nocedal, "An interior point algorithm for large-scale nonlinear programming," SIAM J. Optim., vol.9, no.4, pp.877–900, 1999.
[15] X. Xu, J. Hirokawa, and M. Ando, "Plate-laminated waveguide monipulse slot array antenna with full-corporate-feed in the E-band," IEICE Trans. Commun., vol.E100-B, no.4, pp.575–585, April 2017.
[16] Y. Watarai, M. Zhang, J. Hirokawa, and M. Ando, "Sidelobe suppression in a corporate-feed double-layer waveguide slot array antenna," Proc. Intl. Symp. Antennas Propag., Paper ID: FrD1-5, 2011.
[17] R.W. Haas, D. Brest, H. Mueggenburg, L. Lang, and D. Heimlich, "Fabrication and performance of MMW and SMMW platelet horn arrays," Intl. J. Infrared Milli. Waves, vol.14, no.11, pp.2289–2294, Jan. 1993.
[18] Y. Miura, J. Hirokawa, M. Ando, Y. Shibuya, and Y. Yoshida, "Double-layer full-corporate-feed hollow-waveguide slot array antenna in the 60-GHz band," IEEE Trans. Antennas Propag., vol.59, no.8, pp.2844–2851, Aug. 2011.

Ryotaro Ohashi was born in Shizuoka, Japan. He received the B.S. and M.S. degrees in electrical and electronic engineering from the Tokyo Institute of Technology, Tokyo, Japan, in 2016 and 2018, respectively. He is currently with Research and Development Center, Mitsubishi Electric Corporation, Tokyo, since 2018.

Takashi Tomura was born in Sendai, Japan. He received the B.S., M.S. and D.E. degrees in electrical and electronic engineering from the Tokyo Institute of Technology, Tokyo, Japan, in 2008, 2011 and 2014, respectively. He was a Research Fellow of the Japan Society for the Promotion of Science (JSPS) in 2013. From 2014 to 2017, he worked at Mitsubishi Electric Corporation, Tokyo and was engaged in research and development of aperture antennas for satellite communications and radar systems. From 2017 to 2019, he was a Specially Appointed Assistant Professor at the Tokyo Institute of Technology, Tokyo. He is currently an Assistant Professor there. His research interests include electromagnetic analysis, aperture antennas and planar waveguide slot array antennas. Dr. Tomura received the Best Student Award from Ericsson Japan in 2012 and the IEEE AP-S Tokyo Chapter Young Engineer Award in 2015 and Young Researcher Award from IEICE technical committee on antennas and propagation in 2018. He is a member of the IEEE.

Jiro Hirokawa (S'89-M'90-SM'03-F'12) received the B.S., M.S. and D.E. degrees in electrical and electronic engineering from Tokyo Institute of Technology (Tokyo Tech), Tokyo, Japan in 1988, 1990 and 1994, respectively. He was a Research Associate from 1990 to 1996 and an Associate Professor from 1996 to 2015 at Tokyo Tech. He is currently a Professor there. He was with the antenna group of Chalmers University of Technology, Gothenburg, Sweden, as a Postdoctoral Fellow from 1994 to 1995. His research area has been in slotted waveguide array antennas and millimeter-wave antennas. He received IEEE AP-S Tokyo Chapter Young Engineer Award in 1991, Young Engineer Award from IEICE in 1996, Tokyo Tech Award for Challenging Research in 2003, Young Scientists' Prize from the Minister of Education, Cultures, Sports, Science and Technology in Japan in 2005, Best Paper Award in 2007 and a Best Letter Award in 2009 from IEICE Communications Society, and IEICE Best Paper Award in 2016 and 2018. He is a Fellow of IEICE.